FEBS Open Bio 2 (2012) 51–55

journal homepage: www.elsevier.com/locate/febsopenbio

MAP kinases bind endothelial nitric oxide synthase

Carol A. Chrestensen [a], Jonathan L. McMurry [a], John C. Salerno [b,*]

[a] Department of Chemistry & Biochemistry, Kennesaw State University, Kennesaw, GA 30144-1203, USA
[b] Department of Biology, Kennesaw State University, Kennesaw, GA 30144-1203, USA

ARTICLE INFO

Article history:
Received 8 December 2011
Revised 28 January 2012
Accepted 15 February 2012

Keywords:
Nitric oxide synthase
MAP kinase
ERK
p38
Optical biosensing

ABSTRACT

Endothelial nitric oxide synthase (eNOS) contains a motif similar to recognition sequences in known MAPK binding partners. In optical biosensing experiments, eNOS bound p38 and ERK with ~100 nM affinity and complex kinetics. Binding is diffusion-limited ($k_{on} \sim .15 \times 10^6\ M^{-1}\ s^{-1}$). Neuronal NOS also bound p38 but exhibited much slower and weaker binding. p38-eNOS binding was inhibited by calmodulin. Evidence for a ternary complex was found when eNOS bound p38 was exposed to CaM, increasing the apparent dissociation rate. These observations strongly suggest a direct role for MAPK in regulation of NOS with implications for signaling pathways including angiogenesis and control of vascular tone.

1. Introduction

Kinases of the MAPK family are central nodes in stress activated signaling networks regulating gene expression in response to environmental changes, inflammatory cytokines, and other signals. ERK1/2, p38 and eNOS-generated NO are involved in processes such as angiogenesis, ischemia-reperfusion and insulin response [1–10]. Experimental evidence indicates that ERK1/2 phosphorylates eNOS in a bradykinin-sensitive ERK1/2-AKT-eNOS-Raf-1 complex in BAECs [11]. p38 is stimulated by upstream kinases via several pathways and activates a broad spectrum of downstream kinases, including MAPKAP kinases 2 and 3 and numerous transcription factors such as ATF1/2 and MEF2A [3,12]. Many binding partners for ERK, p38 and JNK contain a basic recognition site within the D-site (Fig. 1) that facilitates interaction between MAP kinases and other signaling components [1–4,12].

The canonical binding site for recognition by MAP kinases is KKRxxxLxI, but considerable variation from this motif has been postulated to facilitate recognition by a helix and neighboring regions on MAPKs that bear an array of acidic and hydrophobic residues. Among several alternatives, Enslena et al. proposed that $(R/K)_2$-$(x)_{2-6}$-(L/I) × (L/I) is a more general motif [13]. Sharrocks et al. presented an even more general scheme for recognition of substrates by MAP kinases involving a multibasic region, an LxL region, and flanking C and N terminal hydrophobic residues; at least two of these four determinants were present in all sequences considered [14]. More recently a series of peptides based on putative recognition sites has been used to probe the specificity of a variety of MAP kinases. Variations within the D site contribute to, but do not completely account for, differential binding of related substrates to JNK, ERK and p38 type kinases, all of which recognize these motifs [4].

The endothelial nitric oxide synthase (eNOS) is an important signal generator involved in the control of vascular tone, insulin secretion, and angiogenesis [6–10]. The primary controller of eNOS is displacement of an autoinhibitory element by Ca^{+2}/CaM (calcium/calmodulin) [15], but eNOS is also regulated by several kinases acting at different sites to activate or inhibit NO production [16–18]. eNOS regulation also involves targeting to different compartments via myristolation, palmitoylation and protein–protein interactions. Some of the activating phosphorylation sites are within the autoinhibitory element (S617 and S633 in bovine eNOS), and are phosphorylated by PKA and AKT.

The autoinhibitory element contains a conserved region common to CaM regulated NOS enzymes; this includes the phosphorylation sites and a helical region that forms hydrogen bonds with the FMN binding domain and with the two domain dehydrogenase unit with which it is associated in the available crystal structure

Abbreviations: AI, autoinhibitory element of nitric oxide synthase; Akt, v-akt murine thymoma viral oncogene homolog 1 (a.k.a, protein kinase B); ATF, activating transcription factor; BAEC, bovine aortic endothelial cells; CaM, calmodulin; eNOS, endothelial nitric oxide synthase; ERK1/2, mitogen activated protein kinase 1 and 2; MEF, myocyte enhancer factor; MK or MAPKAP kinase, mitogen activated protein kinase activated protein kinase; nNOS, neuronal nitric oxide synthase; PKA, protein kinase A

* Corresponding author. Address: Department of Biology, MB #1202, 1000 Chastain Rd., Kennesaw, GA 30144, USA. Fax: +1 770 423 6625.
E-mail address: jsalern3@kennesaw.edu (J.C. Salerno).

2211-5463/$36.00
doi:10.1016/j.fob.2012.02.002

Fig. 1. Alignment of the pentabasic sequence (bold) in eNOS and the aligned region in nNOS and with the D sites of MK2-B, MK3, and MKK6. The classic D site sequence is characterized by (K/R_{2-3}- X_{1-6}-φ-X-φ) (Ref. [4]), is bolded and underlined in the MKK6 sequence. MK2-B and MK3 lack the hydrophobic portion of the D site, similar to eNOS. All sequences are human unless otherwise designated; the sequence corresponding to the recognition region is essentially invariant within each group of mammalian kinase and NOS orthologs.

[19]. The C terminal half of the autoinhibitory element is not conserved at the protein level because of local frame shifts which generated a unique pentabasic sequence in mammalian eNOS. As shown in Fig. 1, the corresponding region of nNOS contains only two basic residues, although there are other basic residues, notably a triplet nearby in the canonical calmodulin-binding motif.

Biosensor experiments provide a powerful and versatile probe of protein–protein interactions, allowing verification of predicted binding and quantitative description of affinity and kinetics of binding and release. Our recent work utilized optical biosensing to elucidate calcium dependent changes to the rates and affinity of calmodulin binding to NOS [20]. Here we show that very compact versions of the D site can be detected and bind with high affinity to MAP kinases such as p38 and ERK1/2. In particular, ERK1/2 binds eNOS but not nNOS and p38 strongly binds to endothelial nitric oxide synthase, but makes a much weaker complex with the neuronal isoform, consistent with the recognition of a pentabasic sequence in eNOS by p38. p38-eNOS binding is inhibited and release stimulated by CaM, suggesting a weak ternary complex. Inhibition of eNOS by p38 is consistent with partial competition with CaM.

2. Materials and methods

NOSs were expressed and purified as described [21–23]. Heme and flavin content were estimated spectrophotometrically, and activity assayed by following NADPH consumption at 340 nm [22,23]. Assays of eNOS NO synthase activity and cytochrome c reduction were performed essentially as described [24,25]. The concentration of CaM was reduced to 0.6 μM because of potential competition between CaM and p38. Phosphorylated His-p38 was expressed as described previously [26] and purified using Talon™ resin as directed by the manufacturer. ERK-2 was purchased from PROSPEC (New Jersey). All biolayer interferometry [27] measurements were made on a ForteBio (Menlo Park, CA) Octet QK biosensor using streptavidin sensors. Assays were performed in 200 μL volumes at 25 °C. p38 and ERK were biotinylated as previously described [20]. Biotinylated kinases were loaded onto sensors for 600 s. After establishing baseline response, kinases were exposed to analyte eNOS or nNOS at a range of concentrations. Baseline, association and dissociation phases were all performed in NOS buffer (10 mM phosphate, pH 7.5, 100 mM NaCl, 10% glycerol, 0.005% surfactant P-20, 10 μM $CaCl_2$). Association and dissociation were monitored as nm shift. Nonspecific binding of analytes to sensors without ligand was negligible and so was not subtracted.

Binding and release of analyte was simulated using standard kinetics approaches [20]. A single first order model generated acceptable simulations for only the first 30 s of binding, but good quality fits were obtained using two components with either sequential (A+B↔C↔D) or parallel (A+B↔C; D+B↔E) models. Sequential binding was modeled at each analyte concentration with pseudo first order rate constants k_1 and k_2 for the forward and reverse reactions of the initial step and k_3 and k_4 for the forward and reverse rate constants of the second step. Binding curves were calculated numerically and forward and reverse rate constants extracted by simulation at all analyte concentrations examined. Parallel model simulation of the forward reactions was done using summed exponentials; the observed pseudo first order rate constant k_{obs} is then the sum of the forward and reverse rates. In both cases the second order rate constant is the product of analyte concentration and pseudo first order forward rate constant k_1.

3. Results

3.1. eNOS binds to p38

In Fig. 2A trace a shows binding of eNOS to tethered p38. Binding is rapid; an initial component accounts for about 2/3 of the signal and has a half time of ~10 s. A second, slower component appears to represent changes in protein conformation on the sensor. After 300 s, the sensor was immersed in buffer only; dissociation of about 25% of the rapid phase binding was observed, consistent with conversion of the remaining complex to a slowly dissociating form in the second phase of association. After dissociation in buffer, the sensor was moved to buffer containing CaM. Dissociation was still incomplete, but significantly more rapid and extensive. We regard the rapid phase of association as representative of potentially physiologically relevant events; very slow conformational changes of protein associated with the sensor surface likely represent partial unfolding or aggregation.

Trace b shows the binding of nNOS to p38. The low amplitude of the signal compared to eNOS indicates that binding is an order of magnitude weaker, and binding is 30-fold slower. It is important to understand that in trace a eNOS is present at saturating concentrations, while the same concentration of nNOS is below the K_d; similar binding of eNOS can be obtained at concentrations about thirty fold lower (see titration in Fig. 2). Weak association of nNOS to p38 may be through basic residues in the AI or the CaM binding region, or may represent a different mode of interaction.

Mutants of eNOS have been previously studied in which the control elements have been deleted [28]. Binding of an deletion mutant in which the autoinhibitory element has been removed to p38 is comparable to the binding of nNOS, but since the nonspecific binding of the eNOS mutant is somewhat greater than that of wild type enzymes, it is not possible to draw more detailed conclusions about weak secondary binding sites at this time. The results are consistent with the behavior of nNOS.

Trace c shows p38 immersed in eNOS as in trace a except that excess Ca^{+2}/CaM was present during association. CaM abolishes binding, suggesting that binding sites overlap, consistent with recognition of the pentabasic motif. p38-eNOS interaction can also be observed with eNOS as ligand and p38 as free analyte (data not shown). The signal is much smaller; this is expected because eNOS is a large protein (dimer molecular weight ~260 kDa) and p38 is much smaller (MW ~ 41 kDa). Inhibition by CaM was also observed. Reversibility of ligand and analyte demonstrates that the interaction is not an artifact of immobilization.

Fig. 2B shows concentration dependence of eNOS binding to p38. Simulation with two components produces good fits; a sequential fit is shown, but good fits can also be obtained with two parallel components. The rapid association phase, most likely to be physiologically relevant, is insensitive to choice of model. Note that the magnitude and rate of eNOS binding that most

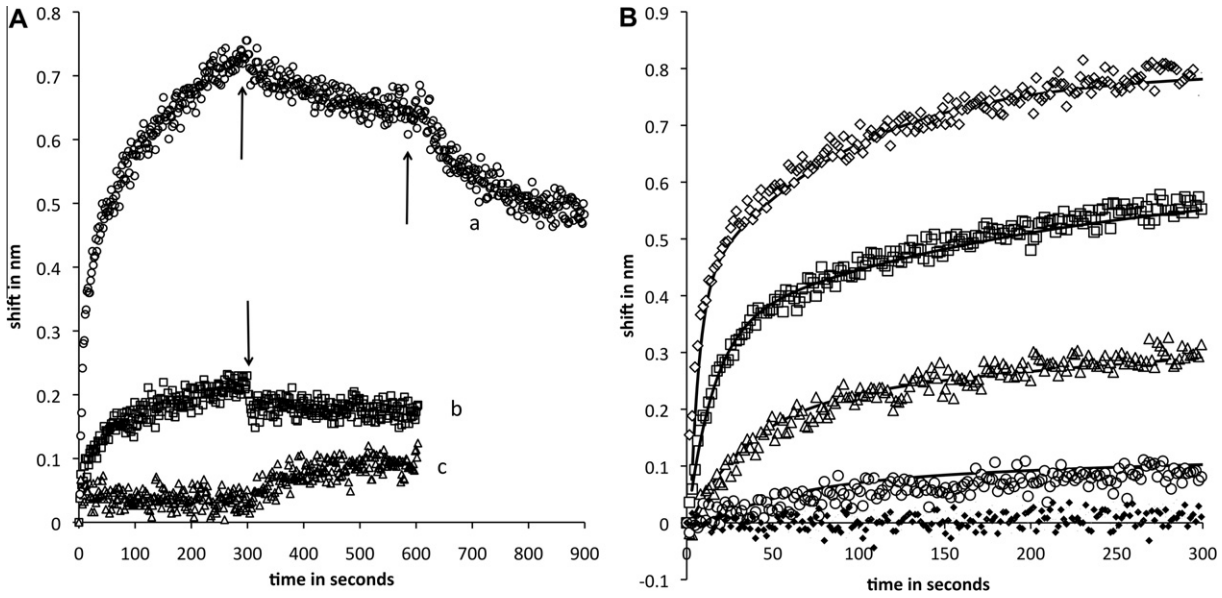

Fig. 2. (A) Sensorgrams of eNOS and nNOS binding to p38. Immobilized p38 was immersed in 696 nM NOS at time 0. Binding was measured for 300 s followed by transfer to buffer only and monitoring of dissociation for 300 s. Trace a (circles), eNOS binding with an additional step in which the tip was moved into buffer with 1 μM CaM after initial dissociation. Trace b (squares), nNOS binding. Trace c (triangles), eNOS pre-equilibrated with a fourfold molar excess of CaM prior to immersion of p38. Arrows indicate movement of sensors from association to dissociation or dissociation to CaM-containing buffer. (B) Sensorgrams of eNOS concentration course. eNOS concentrations in nM units were 696 (open diamonds), 232 (squares), 77 (triangles), 26 (circles) and 0 (black diamonds). Fits to a two-component sequential model are shown as solid lines. Dissociation phases were similar to trace a in Fig. 1. Kinetics parameter sets for successive traces in order of decreasing eNOS were 0.1, 0.01, .006, .001; 0.03, 0.01, 0.0002, 0.001; 0.0008. 0.01, 0.006, 0.001; 0.0025, 0.01, 0.0002, 0.001 in sec-1 for k_1, k_2. k_3, and k_4.

closely match the binding of nNOS in Fig. 1B are obtained at concentrations more than an order of magnitude lower.

Rapid binding is first order with respect to analyte (varied during titration), and the simulations are pseudo-first order with respect to immobilized ligand. Because the analyte is present in great excess, the observed binding kinetics are first order (in immobilized ligand) at each analyte concentration. At high eNOS concentrations the rate of binding (k_1) is much faster than the rate of release (k_2), hence the apparent rate constant $k_{obs} \sim k_1$. The pseudo first order reaction rate at 232 nM eNOS is 0.03 ± 003 s^{-1}, corresponding to a diffusion-limited rate constant of $0.13 \pm .01 \times 10^6$ M^{-1} s^{-1}. K_d for eNOS binding to p38 is k_2/k_1, approximately 80 ± 10 nM.

As shown in Fig. 2A, dissociation of eNOS from p38 is incomplete. This is not due to attainment of equilibrium in the rapid binding phase, because so little eNOS is bound to the sensor that full release would not produce a concentration in the dissociation buffer consistent with observable binding. We interpret these results in terms of a sequential model in which the complex on the sensor is converted to a slowly released form. This process, occurring on the sensor over a time scale of several minutes, is unlikely to be biologically significant, but modeling it improves our understanding of the fast phase.

3.2. eNOS binds to ERK

Fig. 3A shows similar experiments demonstrating the binding of eNOS, but not nNOS, to ERK-2. The concentration dependence of eNOS binding to ERK-2 is shown in Fig. 3B. The concentration dependence is similar to that of the binding of eNOS to p38. The apparent K_d in the single component fit shown is about twice that measured for p38, but the data are consistent with K_d values as small as 90 nM (140 ± 50 nM). A single kinetics component produces suitable fits for the initial 100 s of binding. Rapid binding is first order with respect to the analyte, and at each analyte concentration the observed kinetics are pseudo first order as in Section 3.1. The pseudo first order reaction rate at 100 nM eNOS is 0.125 ± 0.025 s^{-1}, corresponding to a diffusion-limited rate constant of $0.125 \pm 0.025 \times 10^6$ M^{-1} s^{-1}. Low amplitude, likely due to low binding activity of ligand, prevented accurate determination of off rates. Steady state analysis (Fig. 3C) of the binding in Fig. 3B yielded a K_d of 160 nM.

The effect of p38 binding on eNOS activity was investigated using the cytochrome c reduction assay for electron transfer and the hemoglobin capture assay for NO production. There was no significant effect on cytochrome c reduction. Weak inhibition of NO formation by 1 μM p38 in the presence of 0.6 μM CaM was observed; NO production was reduced by an average of 30%. This is consistent with competition between p38 and CaM, assuming that CaM is the stronger ligand as indicated in biosensor experiments. The protein–protein interaction alone does not appear to significantly affect eNOS activity; experiments investigating phosphorylation events are in progress.

3.3. Discussion

We demonstrate that p38 and ERK-2 bind eNOS with high affinity and bind nNOS only weakly or not at all, supporting the hypothesis that the pentabasic sequence in the autoinhibitory element of eNOS, but not nNOS, is recognized by map kinases. Competition with CaM provides additional support for the pentabasic sequence as a MAP kinase target since these elements are proximally located in the three dimensional structure [19]; displacement of the AI by CaM is the primary activating event in both eNOS and nNOS.

The rapid binding and high affinity observed suggest but do not prove that the proteins associate physiologically. Affinity of the established physiologically relevant MK2B-p38 interaction is 6.4 nM [29], comparing well with eNOS-p38 affinity. Physiological p38-eNOS binding would have great potential in mediating signaling pathways known to involve both eNOS and p38. Other kinases might associate with the p38-eNOS complex rather than act as free intermediates. Trafficking of eNOS to cellular compartments is established [16–18], providing opportunity for differential interaction with p38 in some cell states. Numerous papers have

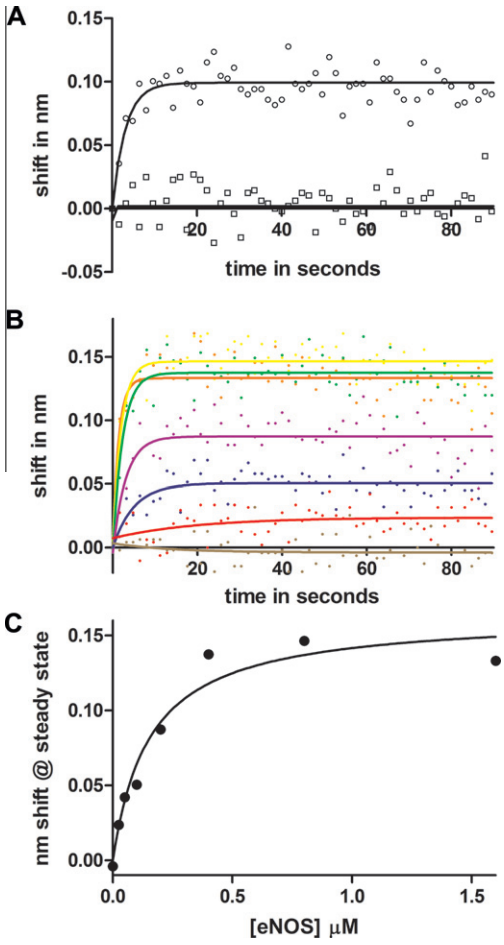

Fig. 3. (A) Association phase of eNOS and nNOS binding to ERK-2. Immobilized ERK2 was immersed in 200 nM NOS at time 0. Trace a (circles), eNOS binding. Trace b (squares), nNOS binding. Solid lines indicate fits to a single exponential. (B) sensorgrams of eNOS concentration course. eNOS concentrations in nM units were 1.6 μM (yellow), 0.8 μM (green), 0.4 μM (orange), 0.2 μM (purple), 0.1 μM (blue), 25 nM (red) and 0 (brown). Solid lines indicate fits to a single exponential. (C) plot of steady state amplitude against eNOS concentration. The fit shown is for K_d = 160 nM.

provided evidence that MAP kinase pathways are involved in regulating both the expression and phosphorylation state of eNOS; some of these pathways inhibit and others activate NO synthesis (e.g., [30,31]) strongly suggesting a mixture of mechanisms that include pathway mediated effects and direct effects (e.g., direct phosphorylation of eNOS by ERK or p38, or activation of an intermediate activating kinase such as AKT in a multiprotein signaling complex).

Available evidence demonstrates that ERK directly phosphorylates eNOS in BAECs, and forms complexes with eNOS and additional components [11]. These complexes are likely to be mediated at least in part by the interactions studied here. We point out that the location of the pentabasic motif, adjacent to the PKA phosphorylation site S633, suggests a mechanism of interaction between modes of inactivation and activation on the enzyme. Recently we directly confirmed inhibition of CaM binding after PKC phosphorylated T495, adjacent to the tribasic motif directly at the start of the CaM canonical target [20]. It is of interest that the MAPK binding site is located in the AI adjacent to a comparable phosphorylation site; the MAPK site exposure is increased by AI displacement but MAPK competes with CaM, and the MAPK binding is positioned to interact with both PKA and AKT phosphorylation sites.

An alternative possibility with broader implications would involve additional partners. The pentabasic sequence of eNOS is recognized by a binding partner in mitochondria [32]. Similar elements are involved in nuclear trafficking. It is easy to envision a system of alternating partners bearing base-rich sequences and their recognition sites that would enable kinases activated by MAP kinases to interact with partners and in turn, eNOS. Such interactions could create a phosphorylation cascade, but could also be the basis for inhibition. We are now investigating the potential of eNOS-MAPK interactions for enhancement of eNOS phosphorylation and inhibition of MAPKAP-2/3 kinases.

3.4. Conclusions

The endothelial nitric oxide synthase binds MAP kinases at a pentabasic site in the unconserved region of the autoinhibitory insertion associated with the eNOS FMN binding domain. No potential MAPK phosphorylation sites are associated with this region in eNOS, but there are many good candidates elsewhere in the eNOS structure that may be accessible to a kinase bound at the pentabasic site. MAP kinases bind eNOS, but not homologs lacking the pentabasic site, with ~100 nM affinity and a forward rate constant of $\sim 1.3 \times 10^5\ M^{-1}\ s^{-1}$. Calmodulin forms a ternary complex that weakly promotes dissociation of p38 from eNOS. The eNOS-MAP kinase interaction may provide a scaffold for the formation of larger complexes with additional components, including Akt and Raf-1.

Acknowledgements

We thank Raj Razdan and Emily Rye for expert technical assistance. This work was supported by NSF 1020261 and Research Corporation CC6942 (to C.A.C.), NIH 1R15GM083317 (J.L.M.) and NIH 3R15GM080701-01 and NSF 0950920 (J.C.S.).

References

[1] Cargnello, M. and Roux, P.P. (2011) Activation and function of the MAPKs and their substrates, the MAPK-activated protein kinases. Microbiol. Mol. Biol. Rev. 75, 50–83.
[2] Cuadrado, A. and Nebreda, A.R. (2010) Mechanisms and functions of p38 MAPK signaling. Biochem. J. 429, 403–417.
[3] Zarubin, T. and Han, J. (2005) Activation and signaling of the p38 MAP kinase pathway. Cell Res. 15, 11–18.
[4] Bardwell, A.J., Frankson, E. and Bardwell, L. (2009) Selectivity of docking sites in MAPK kinases. J. Biol. Chem. 284, 13165–13173.
[5] Gaestel, M. (2008) Specificity of signaling from MAPKs to MAPKAPKs: kinases' tango nuevo. Front. Biosci. 13, 6050–6059.
[6] Ignarro, L.J., Buga, G.M., Wood, K.S., Byrns, R.E. and Chaudhuri, G. (1987) Endothelium-derived relaxing factor produced and released from artery and vein is nitric oxide. Proc. Natl. Acad. Sci. 84, 9265–9269.
[7] Furchgott, R. (1988) Studies in relaxation of rabbit aorta by sodium nitrite: the basis for the proposal that the acid activaible factor from bovine retractor penis is inorganic nitrite, Vasodilation: Vascular Smooth Muscle Peptides, Autonomic Nerves and Endothelium, pp. 401–404, Raven Press, New York.
[8] Papapetropoulos, A., Garcia-Cardena, G., Madri, J.A. and Sessa, W.C. (1997) Nitric oxide production contributes to the angiogenic properties of vascular endothelial growth factor in human endothelial cells. J. Clin. Invest. 100, 3131–3139.
[9] Corbett, J.A., Sweetland, M.A., Wang, J.L., Lancaster Jr., J.R. and McDaniel, M.L. (1993) Nitric oxide mediates cytokine-induced inhibition of insulin secretion by human islets of Langerhans. Proc. Natl. Acad. Sci. 90, 1731–1735.
[10] Henningsson, R., Salehi, A. and Lundquist, I. (2002) Role of nitric oxide synthase isoforms in glucose-stimulated insulin release. Am. J. Physiol. 283, C296–304.
[11] Bernier, S.G., Haldar, S. and Michel, T. (2000) Bradykinin-regulated interactions of the mitogen-activated protein kinase pathway with the endothelial nitric-oxide synthase. J. Biol. Chem. 275, 30707–30715.
[12] Roux, P.R. and Blenis, J. (2004) ERK and p38 MAPK-activated protein kinases: a family of protein kinases with diverse biological functions. Microbiol. Mol. Biol. Rev. 68, 320–344.
[13] Enslena, H. and Davis, H.J. (2001) Regulation of MAP kinases by docking domains. Biol. Cell 93, 5–14.
[14] Sharrocks, A.D., Yang, S.-I. and Galanis, A. (2000) Docking domains and substrate specificity determination for MAP kinases. TIBS 25, 448–453.

[15] Salerno, J.C., Harris, D.E., Irizarry, K., Patel, B., Morales, A.J., Smith, S.M., Martasek, P., Roman, L.J., Masters, B.S., Jones, C.L., Weissman, B.A., Lane, P., Liu, Q. and Gross, S.S. (1997) An autoinhibitory control element defines calcium-regulated isoforms of nitric oxide synthase. J. Biol. Chem. 272, 29769–29777.
[16] Boo, Y.C., Kim, H.J., Song, H., Fulton, D., Sessa, W. and Jo, H. (2006) Coordinated regulation of endothelial nitric oxide synthase activity by phosphorylation and subcellular localization. Free Rad. Biol. Med. 41, 144–153.
[17] Mount, P.F., Kemp, B.E. and Power, D.A. (2007) Regulation of endothelial and myocardial NO synthesis by multi-site eNOS phosphorylation. J. Mol. Cell. Cardiol. 42, 271–279.
[18] Fulton, D., Gratton, J.P. and Sessa, W.C. (2001) Post-translational control of endothelial nitric oxide synthase: why isn't calcium/calmodulin enough? J. Pharmacol. Exper. Ther. 299, 818–824.
[19] Garcin, E.D., Bruns, C.M., Lloyd, S.J., Hosfield, D.J., Tiso, M., Gachhui, R., Stuehr, D.J., Tainer, J.A. and Getzoff, E.D. (2004) Structural basis for isozyme-specific regulation of electron transfer in nitric-oxide synthase. J. Biol. Chem. 279, 37918–37927.
[20] McMurry, J.L., Chrestensen, C.A., Scott, I.M., Lee, E.W., Rahn, A.M., Johansen, A.M., Forsberg, B.J., Harris, K.D. and Salerno, J.C. (2011) Rate, affinity and calcium dependence of nitric oxide synthase isoform binding to the primary physiological regulator calmodulin. FEBS J. 278, 4943–4954.
[21] Gerber, N.C. and Ortiz de Montellano, P.R. (1995) Neuronal nitric oxide synthase. Expression in *Escherichia coli*, irreversible inhibition by phenyldiazene, and active site topology. J. Biol. Chem. 270, 17791–17796.
[22] Roman, L.J., Sheta, E.A., Martasek, P., Gross, S.S., Liu, Q. and Masters, B.S. (1995) High- level expression of functional rat neuronal nitric oxide synthase in *Escherichia coli*. Proc. Natl. Acad. Sci. 92, 8428–8432.
[23] Martasek, P., Liu, Q., Liu, J., Roman, L.J., Gross, S.S., Sessa, W.C. and Masters, B.S. (1996) Characterization of bovine endothelial nitric oxide synthase expressed in *E. coli*. Biochem. Biophys. Res. Commun. 219, 359–365.
[24] Gross, S.S. (1996) Microtiter plate assay for determining kinetics of nitric oxide synthesis. Methods Enz. 268, 159–168.
[25] Newman, E., Spratt, D.E., Mosher, J., Cheyne, B., Montgomery, H.J., Wilson, D.L., Weinberg, J.B., Smith, S.M., Salerno, J.C., Ghosh, D.K. and Guillemette, J.G. (2004) Differential activation of nitric-oxide synthase isozymes by calmodulin-troponin C chimeras. J. Biol. Chem. 279, 33547–33557.
[26] Chrestensen, C.A., Schroeder, M.J., Shabanowitz, J., Hunt, D.F., Pelo, J.W., Worthington, M.T. and Sturgill, T.W. (2004) MAPKAP kinase 2 phosphorylates tristetraprolin on in vivo sites including Ser178, a site required for 14–3-3 binding. J. Biol. Chem. 279, 10176–10184.
[27] Abdiche, Y., Malashock, D., Pinkerton, A. and Pons, J. (2008) Determining kinetics and affinities of protein interactions using a parallel real-time label-free biosensor, the Octet. Anal. Biochem. 377, 209–217.
[28] Roman, L.J. and Masters, B.S. (2006) Electron transfer by neuronal nitric-oxide synthase is regulated by concerted interaction of calmodulin and two intrinsic regulatory elements. J. Biol. Chem. 281, 23111–23118.
[29] Lukas, S.M., Kroe, R.R., Wildeson, J., Peet, G.W., Frego, L., Davidson, W., Ingraham, R.H., Pargellis, C.A., Labadia, M.E. and Werneburg, B.G. (2004) Catalysis and function of the p38 alpha MK2a signaling complex. Biochemistry 43, 9950–9960.
[30] Kumar, V.B., Viji, R.I., Kiran, M.S. and Sudhakaran, P.R. (2009) Negative modulation of eNOS by laminin involving post-translational phosphorylation. J. Cell Physiol. 219 (1), 123–131.
[31] Kan, W.H., Hsu, J.T., Ba, Z.F., Schwacha, M.G., Chen, J., Choudhry, M.A., Bland, K.I. and Chaudry, I.H. (2008) P38 MAPK-dependent eNOS upregulation is critical for 17beta-estradiol-mediated cardioprotection following trauma-hemorrhage. Am. J. Physiol. Heart Circ. Physiol. 294, H2627–36.
[32] Gao, S., Chen, J., Brodsky, S.V., Huang, H., Adler, S., Lee, J.H., Dhadwal, N., Cohen-Gould, L., Gross, S.S. and Goligorsky, M.S. (2004) Docking of endothelial nitric oxide synthase (eNOS) to the mitochondrial outer membrane: a pentabasic amino acid sequence in the autoinhibitory domain of eNOS targets a proteinase K-cleavable peptide on the cytoplasmic face of mitochondria. J. Biol. Chem. 279, 15968–15974.